*Journal of Enzyme Inhibition*, Vol. 16, pp. 401–416
Reprints available directly from the publisher
Photocopying permitted by license only





# Enantioselectivity of Some 1-[(Benzofuran-2-yl) phenylmethyl] imidazoles as Aromatase ($P450_{AROM}$) Inhibitors

G.A. KHODARAHMI[a], C.A. LAUGHTON[b], H.J. SMITH[a,*] and P.J. NICHOLLS[a]

[a]*The Welsh School of Pharmacy, Cardiff University, Cardiff CF10 3XF, UK;* [b]*School of Pharmaceutical Sciences, University Park, University of Nottingham, Nottingham NG7 2RD, UK*

*(Received 3 July 2001)*

**The enantioselectivity ratio ((+)-:(−)-forms) of three substituted 1-[(benzofuran-2-yl) phenylmethyl] imidazoles as inhibitors of aromatase ($P450_{AROM}$) was 2.16, 12.3 and 1.0 for the 4-methyl-, 4-fluoro- and 4-chloro-substituted compounds, respectively. The (±)-compounds were all >1000 times more potent than (±)-aminoglutethimide ($IC_{50} = 12 \times 10^3$ nM). High potency (5.3–65.0 nM) for all the enantiomers studied is unusual since activity usually resides in one form for chiral inhibitors of $P450_{AROM}$. The 4-methyl derivative was fitted into the model [Furet, P., Batzl, C., Bhatnager, A.S., Francotte, E., Rihs, G. and Lang, M. (1993) *J. Med. Chem.* 36, pp. 1393–1400] for binding of *S*-(−)-fadrazole to the active site and the (*R*)- and (*S*)- forms both gave a good fitting pattern with (*S*)-(−)-fadrazole so accounting for their close activity. Docking of both forms into the active site model for $P450_{AROM}$ [Laughton, C.A., Zvelebil, M.J.J.M. and Neidel, S. (1993) *J. Steroid Biochem. Mol. Biol.* 44, pp. 399–407], using the orientation of (*S*)-(−)-fadrazole, gave similar strong binding along the position of the C and D rings of the steroid substrate and in the hydrophobic cavity below the A/B rings. The site was probed for group size accommodation using the less potent 4-phenyl analogue ($IC_{50}(\pm) = 242$ nM): the (*S*)-form showed restricted access to the region under the A ring due to the extended bulk of the biphenyl group.**

*Keywords*: Aromatase; $P450_{AROM}$; Inhibition; Enantioselectivity; Docking; Modelling

## INTRODUCTION

Aromatase ($P450_{AROM}$), which catalyses the final step in the oestrogen biosynthesis cascade, has been the target for agents in the treatment of breast cancer in women. $P450_{AROM}$ inhibitors have been used as second line therapy after tamoxifen in oestrogen-receptor positive (ER+) women to reduce plasma and breast levels of oestrogen and thus the stimulus to growth of oestrogen-dependent metastases.[1]

The stereochemistry of enzyme inhibitors possessing a chiral centre is usually important

*Corresponding author. Fax: +44-29-20-874149. E-mail: smithhj1@cardiff.ac.uk

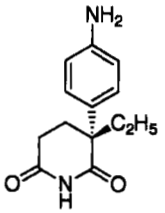

(**1**): (*R*)-(+)-aminoglutethimide

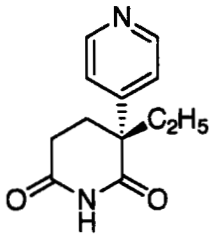

(**2**): (*R*)-(+)-rogletimide

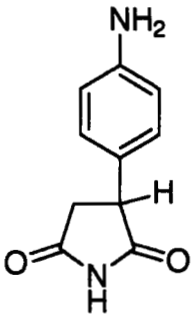

(**3**)

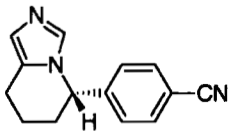

(**4**): (*S*)-(-)-fadrazole

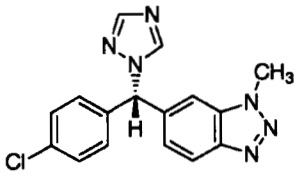

(**5**): (*S*)-(+)-vorozole

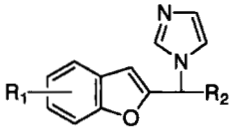

(**6**)

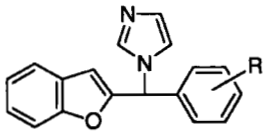

(**7**): R = H
(**8**): R = 4-$CH_3$
(**9**): R = 4-Cl
(**10**): R = 4-F

in determining their *in vitro* potency towards a specific enzyme although *in vivo* the situation may be less clear.[2,3] Aminoglutethimide (**1**, AG) has been a long established inhibitor of $P450_{AROM}$ used clinically as the racemate. The activity lies in the (*R*) (+)-form (38×(*S*) (−) form).[4] Other analogues of AG (**2**), the ring-contracted 3-phenylpyrrolidine-2,5-diones (**3**), the non-selective imidazole antifungals and the potent, selective second and third generation

chiral imidazole and triazole inhibitors (**4**,**5**), show a similar residence of inhibitory potency in just one of the enantiomers.[5]

We have recently resolved a series of substituted 1-(benzofuran-2-yl)-1-(1*H*-imidaz-1-yl)alkanes. The (+)-form of (**6**, $R_1 = 5,7-\text{DiCl}$, $R_2 = CH_3$) was 4.8-fold more potent than the (−)-form and a 12.6-fold similar entantioselectivity was found for (**6**, $R_1 = 2,4-\text{DiBr}$, $R_2 = CH_3$). In the corresponding ethyl series ($R_2 = CH_2CH_3$), the stereoselective ratios were 8.3 and 5.2 for the respective similarly substituted compounds.[6]

We have previously shown[7] that suitably substituted 1-[(benzofuran-2-yl)phenylmethyl]imidazoles (**7**) are potent inhibitors of $P450_{AROM}$ and here we have studied their enantioselectivity as analogues of (**6**, *R* = alkyl). We have resolved, using dibenzoyl tartaric acid (DBT), the (+)- and (−)-forms (as salts) of the 4-methyl (**8**), 4-fluoro (**9**) and 4-chloro (**10**) analogues, examined their enantioselectivity to the enzyme and fitted (**8**) to the model for binding of *S*-(−)-fadrazole to the active site.[8] (**8**) was also fitted to the active site model for aromatase[9] as was the biphenyl analogue (**6**, *R*=Ph−Ph) to probe the steric requirements of the aromatase binding sites.

## MATERIALS AND METHODS

### Chemistry

The reagents used were either general purpose or analytical grade. Solvents for resolution studies were from Fisher Scientific (Loughborough, UK). Melting points were determined with an Electrothermal instrument and are uncorrected. Infra red spectra were determined with a Perkin–Elmer 681 infrared spectrophotometer. Optical rotation was measured on a Bellingham and Stanley polarimeter. $^1$H NMR spectra were determined with a Perkin–Elmer R32 (90 MHz) Spectrophotometer; TMS was used as an internal standard. Elemental analyses were done by the School of Pharmacy, University of London.

The 1-[(benzofuran-2-yl)phenylmethyl]imidazoles (**8**–**10**) were synthesised by the general method of Pestillini *et al.*[10]. The biphenyl analogue (**6**, *R*=Ph−Ph) was a gift from Menarini Recherche.

1-[(Benzofuran-2-yl) (4′-methylphenyl)methyl] -1*H*-imidazole (**8**) was obtained as a pale yellow oil. The hydrochloride salt was formed by bubbling HCl gas into an ether solution (50 ml) of (**8**). Initially a semi-solid was formed, which was separated and washed with acetone to give a white crystalline solid (4.1 g) mp: 189–91°C (mp: 185–186°C)[11] (Found: C, 69.9; H, 5.13; N, 8.17. $C_{19}H_{17}ClN_2O$ requires C, 70,26; H, 5.28; N, 8.62%). $\nu_{max}$: 3100 (Ar, C–H), 2910 (C–H), 1560 (Ph) cm$^{-1}$. $\delta$ 9.25 (1H,s,imidazole 2-H), 7.6–7.2 (11H,m,benzofuran,phenyl and imidazole 4,5-H), 6.8 (1H,s,C–H), 2.33 (3H,s,Ph–$CH_3$).

1-[(Benzofuran-2-yl)(4′-fluorophenyl)methyl]-1*H*-imidazole HCl (**9**) was obtained as white crystals (7.92 g, 27%) mp: 184–186°C (acetone) (mp: 181–182°C).[11] $\nu_{max}$: 3110 (Ar, C–H), 2930 (CH), 1610 (Ph) cm$^{-1}$. $\delta$(DMSO-$d_6$): 9.6 (1H,s, imidazole 2-H), 8.1–7.1 (11H,m, benzofuran and phenyl), 6.9 (1H,s, –CH–).

1-[(Benzofuran-2-yl)(4′-chloro-phenyl)methyl] -1*H*-imidazole HCl (**10**) has been previously described.[3]

### Resolution Studies

#### *Chiral Separation of 1-[(benzofuran-2-yl)(4′-methylphenyl)methyl]-1H-imidazole (8)*

Potassium carbonate (2%, 100 ml) was added to 1-[(benzofuran-2-yl)(4′-methylphenyl)methyl]-1-*H*-imidazole HCl salt (**8**) (2 g, 6.16 mmol) and the mixture was stirred at room temperature for 10 min to give a coagulate, which was then extracted with ether (3 × 40 ml). The combined organic layers were washed with water (3 × 50 ml) and dried ($MgSO_4$). The solvent was evaporated to yield the free base as a pale-yellow oil (1.75 g, 6.07 mmol), which was used for the resolution studies.

### *1-[(Benzofuran-2-yl)(4′-methylphenyl)methyl]-1 H-imidazole Dibenzoyl-D-(+)-tartrate, (8-(+)-DBT)*

Dibenzoyl-D-(+)-tartaric acid (1.05 g, 2.93 mmol) in ether (20 ml) was added to a solution of 1-[(benzofuran-2-yl) (4′-methylphenyl)methyl]-1*H*-imidazole (**8**), (0.84 g, 2.92 mmol) in ether (20 ml) to yield a white solid (1.6 g). To a small amount of the crude solid, a few drops of ethanol was added and then the solution was heated on a water bath to give a clear solution. The solution was cooled and then stirred for 3 h to yield some white crystals, which were used as seed for the next step. Ethanol (2.5 ml) was added to the solid (1.6 g) and the solution was heated until dissolution was completed. After seeding the solution was left at 4°C for 24 h. The resulting solid was filtered off and washed with a few drops of cold ethanol to give white crystals (1.32 g) which were then recrystallised a further six times at room temperature (ethanol) to yield (**8**-(+)-DBT) as white crystals (60 mg overall yield 3.18%) mp: 124–125°C. $[\alpha]_{25}^{D} = +63.77°$ (salt) (1%, methanol). (Found: C, 68.49; H, 4.82; N, 4.45. $C_{37}H_{30}N_2O_9$ requires C, 68.72; H, 4.67; N, 4.33%). The recrystallisation steps were monitored, using HPLC on the released base, after each recrystallisation (Fig. 1).

### *1-[Benzofuran-2-yl)(4′-methylphenyl)methyl]-1 H-imidazole Dibenzoyl-L-(−)-tartrate, (8-(−)-DBT)*

Dibenzoyl-L-(−)-tartaric acid ((−)-DBT) (1.05 g) (1.05 g, 2.93 mmole) in ether (20 ml) was added to a solution of 1-[benzofuran-2-yl)(4′-methylphenyl)methyl]-1*H*-imidazole (**8**) (0.84 g, 2.92 mmol) in ether (20 ml) to give a white precipitate (1.56 g, crude).

Ethanol was added to some of the crude solid to give a clear solution and then after cooling, the solution was put in ice $CO_2$ and the resulting solid was scratched for 15 min and then left overnight at 4°C to yield a white crystalline solid. The remaining solid (1.15 g) was recrystallised (ethanol) a further five times at room temperature to give (**8**-(−)-DBT) as white crystals (20 mg, 1.1%) mp: 124°C. $[\alpha]_{25}^{D} = -63.65°$ (salt) (1%, methanol). (Found: C, 68.63; H, 4.76; N, 4.52. $C_{37}H_{30}N_2O_9$ requires C, 68.72; H, 4.67; N, 4.33%). The recrystallisation steps were monitored, using

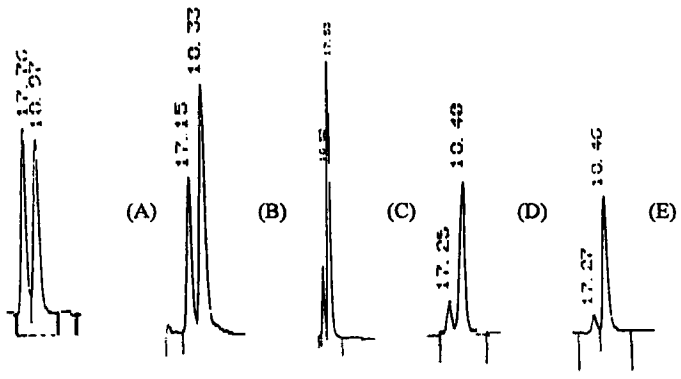


FIGURE 1 Chromatograms for (**8**-DBT)-racemate (A), and recrystallised fractions of (**8**-(+)-DBT) after one, (B), five (C), six (D) and seven (E) recrystallisations.

HPLC on the released base, after each recrystallisation.

### *Chiral Separation of 1-[Benzofuran-2-yl)(4′-fluorophenyl)methyl]-1H-imidazole (9)*

#### *1-[(Benzofuran-2-yl)(4′-fluorophenyl)methyl]-1H-imidazole Dibenzoyl-D-(+)-tartrate, (9-(+)-DBT)*

1-[(Benzofuran-2-yl)(4′-fluorophenyl)methyl]-1-*H*-imidazole-HCl salt (**9**) (2 g, 6.1 mmole) was released as the base as previously described for (**8**) and reacted with dibenzoyl-D-(+)-tartaric acid (2.18 g, 6.1 mmol). The precipitate (2.4 g) after four times recrystallisation (ethanol) gave (**9**-(+)-DBT) as white crystals (70 mg, 1.76%). mp: 134.5–135.5°C. $[\alpha]_{25}^{D} = +62.4°$ (salt) (1%, methanol). (Found: C, 65.01; H, 4.45; N, 4.20 $C_{36}H_{27}FN_2O_9 \cdot H_2O$ requires C, 64.67; H, 4.45; N, 4.20%). The recrystallisation steps were monitored, using HPLC on the released base, after each recrystallisation.

#### *1-[(Benzofuran-2-yl)(4′-fluorophenyl)methyl]-1H-imidazole Dibenzoyl-L-(−)-tartrate, (9-(−)-DBT)*

1-[(Benzofuran-2-yl)(4′-fluorophenyl)methyl] -1*H*-imidazole HCl salt (**9**), (2 g, 6.1 mmol) was released as the base and reacted with dibenzoyl-L-(−)-tartaric acid (2.18 g, 6.1 mmole) as previously described. The precipitate gave (**9**-(−)-DBT) as a white solid (300 mg, 76%) after four times recrystallisation (ethanol). mp:134.5–135.5°C. $[\alpha]_{25}^{D} = -62.5°$ (salt), (1%, methanol), $[\alpha]_{25}^{D} = -24.42°$ (free base) (1%, chloroform). (Found: C, 64.86; H, 4.54; N, 4.08. $C_{36}H_{27}FN_2O_9 \cdot H_2O$ requires C, 64.67; H, 4.37; N, 4.19%. The recrystallisation steps were monitored, using HPLC on the released base, after each recrystallisation.

1-[(Benzofuran-2-yl)(4′-chlorophenyl)methyl]-1*H*-imidazole dibenzoyl-D-(+)- and dibenzoyl-L-(−)-tartrates (**10**-(+)- and (−)-DBT, respectively were previously synthesised by us.[3]

### HPLC of Enantiomers

#### *Instrumentation and Condition for Analysis by HPLC*

A Milton Roy LC system was used consisting of a Model 3000 constantametric pump, a Rheodyne injection unit and a model 3100 variable wavelength spectromonitor. A model CL-4100 computing integrator was used to process the HPLC data. The HPLC column used was an amylose coated silica gel column (Chiralpak AD; 4.6×250 mm, Daicel Chemical LTD) using a precolumn (4.6×50 mm) both packed with identical material (amylose tris(3,5-dimethylphenyl carbamate)). Injection on the column was achieved using a Hamilton syringe (50 µl) into a Rheodyne 20 µl loop. Chromatographic conditions were as follows: Mobile phase, n-hexane:2-propanol:diethylamine (80:20:0.1); Flow rate, 0.7 ml/min; Detector, UV 288 nm; Temperature, ambient; Injection volume, 20 µl; Pressure, 130 psi.

#### *Determination of the Enantiomeric Purity of (+)-1-[(benzofuran-2-yl)(4′-methylphenyl)methyl]-1H-imidazole Dibenzoyl-D-(+)-tartrate(8-(+)-DBT)*

Potassium carbonate (2%, 10 ml) was added to some of the (8-(+)-DBT) obtained after seven recrystallisations from ethanol, and the free base extracted into dichloromethane (2×10 ml). The organic phase was washed with water (2×10 ml) and dried ($MgSO_4$). The solvent was evaporated and the residue was dissolved in the mobile phase (1 ml) and injected into the HPLC.

Figure 1 shows the enantiomeric composition of the chromatograms after successive recrystallisations. The enantiomeric purity of the final recrystallisation of (**8**-(+)-DBT) was (first enantiomer, (−))=10.3% (second enantiomer, (+))=89.7%.

The enantiomeric purity of (−)-1-[(benzofuran-2-yl)(4′-methylphenyl)methyl]-1*H*-imidazole dibenzoyl-L-(−)-tartrate, (8-(−)-DBT) after 6 recrystallistions was (first enantiomer, (−))=97.0%, (second enantiomer, (+))=3.0%.

The enantiomeric purity (+)-1-[(benzofuran-2-yl)(4′-fluorophenyl)methyl]-1*H*-imidazole dibenzoyl-D-(+)-tartrate, (9-(+)-DBT): after 4 recrystallisations was (first enantiomer, (−))=2.53%, (second entantiomer, (+))=97.47%.

The enantiomeric purity of (−)-1-[(benzofuran-2-yl)(4′-fluorophenyl)methyl]-1*H*-imidazole dibenzoyl-L(−)-tartrate, (9-(−)-DBT) was (first enantiomer, (−))=97.43%, (second enantiomer, (+))=2.57%.

## Biochemistry

The compounds in ethanol (10 μl) at a range of concentrations were included in the standard assay for $P450_{AROM}$ of human placental microsomes prepared by the method of Thompson and Siiteri[12] as described by Khodarahmi *et al.*,[6] using [1β-$^3$H]-androstenedione. Control incubations included ethanol (10 μl). Aminoglutethimide was included for comparison. $IC_{50}$ values were calculated from a plot of (% activity remaining) vs log [inhibitor] using Cricket Graph.

The results obtained (Table I) show that the enantiomers have similar activities for the 4-methyl (8-DBT) and 4-chloro (10-DBT)) compounds whereas a 15-fold difference is seen for the 4-fluoro (9-DBT) compound. The interesting point is that both enantiomers for the three analogues are very potent inhibitors.

TABLE I $IC_{50}$ values (nM)* for some 1-[(benzofuran-2-yl)phenylmethyl] imidazoles (salts) as aromatase inhibitors

| | (+) | (−) | (±) |
|---|---|---|---|
| (8-DBT) 4-$CH_3$ | 7.4 | 16.3 | 11.0 |
| (9-DBT) 4-F | 5.3 | 65.0 | 8.6 |
| (10-DBT) 4-Cl | 8.4 | 8.4 | 10.2 |
| AG | | | 12,000 |

* Androstenedione, 0.6 μM. Mean of triplicate estimations <2% of mean.

## Modelling

The molecular modelling studies were conducted using the PIMMS molecular modelling programme (Pimms V1.43, Oxford Molecular Ltd., 1993) running on a Silicon Graphics work station. This software was used to build, manipulate, analyse and display the molecular structures. Energy calculations and conformational analysis were performed using the in-built COSMIC forcefield. The required crystallographic structures were retrieved from the crystal structure search and retrieval database, Cambridge Crystal Data Center, from the chemical data bank system (CDS1) at Daresbury.

### *Molecular Modelling Analysis of (19R)-10-thiiranyl-androst-4-ene-3,17-dione (TAD) and (S)-(−)-fadrozole*

TAD was constructed from the structure of testosterone, retrieved from Daresbury, (refcode TESTON10). The molecular structure of TAD was subjected to an initial optimisation. A low energy structure was then determined by performing a conformational search. The lowest

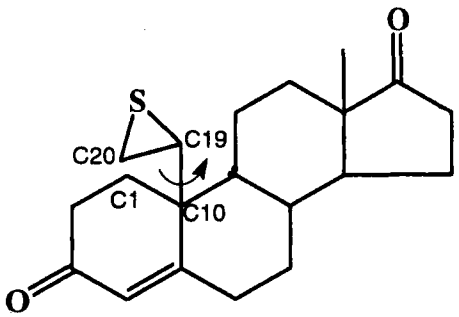


**TAD**

FIGURE 2 Structure of TAD, with definition of the torsion angle $\phi$=C1–C10–C19–C20.

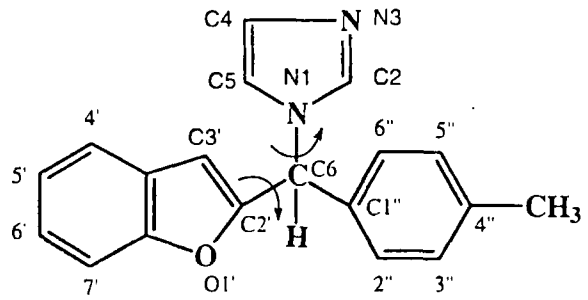


FIGURE 3 Structure of (**8**), and definition of torsion angles $\phi$ and $\psi$, $\phi$ = C(1″)–C(6)–N(1)–C(5) and $\psi$ = C(1″)–C(6)–C(2′)–C(3′).

energy conformation was then selected and its structure optimised, using the optimisation facility in Pimms ($E = 81.59$ kcal/mole, $\phi$ = C1–C10–C19–C20 = 71.51°; Fig. 2) and used for the superimposition studies.

(*S*)-(−)-Fadrozole was retrieved from Daresbury as (*S*)-(−) fadrozole D-(−)-tartrate salt (Furet *et al.* refcode SUKNER).[8] The tartrate part was removed and (*S*)-(−)-fadrozole was then optimised using the default conditions in the Pimms programme and this was used for the modelling studies.

(*R*)-(**8**) was constructed using the benzofuran moiety of 2-acetyl-4,6-dimethoxy benzofuran (refcode CUYRAP) retrieved from Daresbury, and was subjected to an initial minimisation. Conformational analysis of (*R*)-(**8**) was performed by separate rotation about the C(2′)–C(6), N(1)–C(6) and C(1″)–C(6) bonds (see Fig. 3) in 1° increments, and then all bonds at 20° increments to obtain the minimum energy conformer. The minimum energy conformer from this study was subjected to further conformational analysis by rotation about C(2′)–C(6) and N(1)–C(6) bonds in 10° increments in order to define local energy minima.

Analysis of the results from a Ramachandran plot indicated that (*R*)-(**8**) could adopt a wide range of conformations in four distinct oval

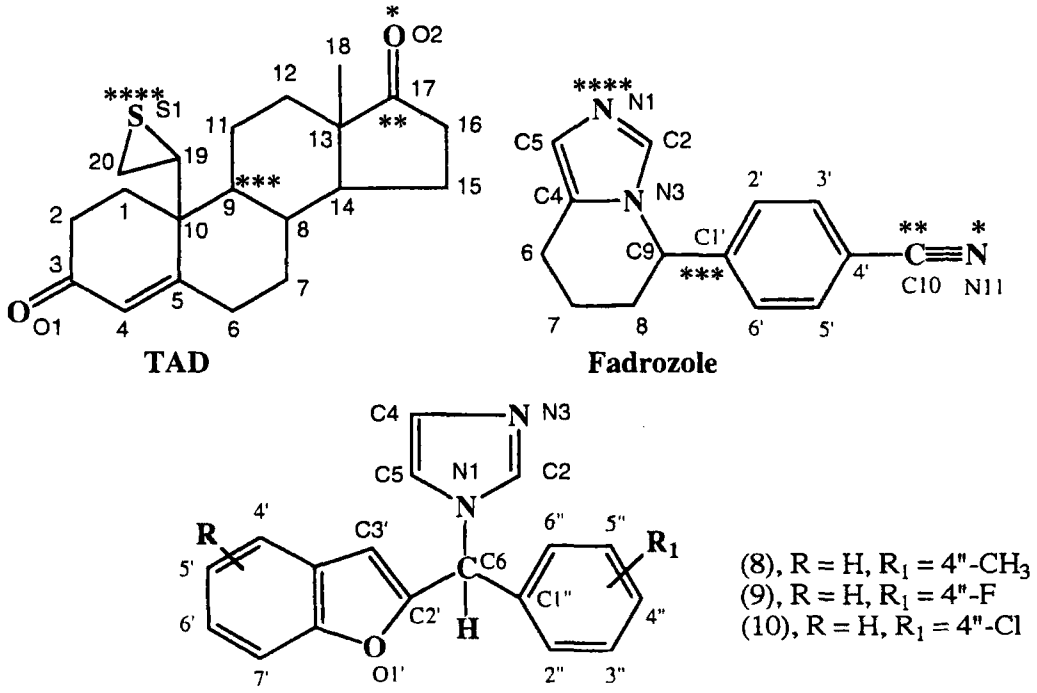


FIGURE 4 Structures of TAD, (*S*)-(−)-fadrozole and 1-[(benzofuran-2-yl) (phenylmethyl)-1*H*-imidazoles showing atom labelling. The pairs of atoms used for superimposition of (*S*)-(−)-fadrozole on TAD are marked *, **, *** and ****.

shape areas of lowest energies which allows the existence of conformations within the approximate ranges of $\phi$ and $\psi$: (L1) $\phi \cong 110-180°$ and $\psi \cong 20-160°$; (L2) $\phi \cong 150-180°$ and $\psi \cong 120-(-70°)$; (L3) $\phi \cong -80-(-30°)$ and $\psi \cong 100-180°$, $150-(-180°)$; (L4) $\phi \cong -80-(-60°)$ and $\vartheta \cong 20-60°$.

The final conformer (from the local minima L1, was taken and included in the fitting studies.

(*S*)-(−)-Fadrozole was superimposed on TAD, using the approach of Furet *et al.*[8] The pairs of atoms used for superimposition are marked (*, **, ***, and ****) (see Fig. 4). The final conformer of (*R*)-(**8**) from the local minima (L1) was superimposed on (*S*)-(−)-fadrozole (which was fitted on TAD) by superimposing all the atoms of its imidazole on the corresponding atoms of the imidazole ring of (*S*)-(−)-fadrozole. The matched structures are shown in Fig. 5.

Looking at the structures, the 4′-methylphenyl substituent of (*R*)-(**8**) was extended along the cyanophenyl ring of (*S*)-(−)-fadrozole or the rings C and D of TAD, while the benzofuran dipped below the A/B rings. The distance between the N3 atom of (*R*)-(**8**) and N1 of (*S*)-(−)-fadrozole or the S1 atom of TAD was about 0.35 Å. The low energy conformers of (*R*)-(**8**) from other local energy minima i.e. L2, L3 and L4 showed almost the same fitting scheme.

Superimposition of the final conformer of (*S*)-(**8**) from the conformational analysis was achieved using the pairs of atoms described previously for (+)-(**8**) and the matched structures is shown in Fig. 6. The distance between the N1 of (−)-(8) and N3 of (*S*)-(−)-fadrozole or S1 of TAD was about 0.35 Å.

The analogues (*R*)-(**9**) and (*R*)-(**10**) were superimposed on (*S*)-(−)-fadrozole separately and gave results similar to (*R*)-(**8**) (not shown).

The results from these modelling studies indicated a very good fitting pattern for both (+)- and (−)-enantiomers. For the (+)-enantiomers the substituted phenyl group extended along the C and D rings of TAD and the cyanophenyl ring of fadrozole and the benzofuran ring dipped below the rings A/B of TAD into the proposed hydrophobic pocket of the enzyme.[9] The (−)-enantiomers were superimposed on fadrozole by having the benzofuran

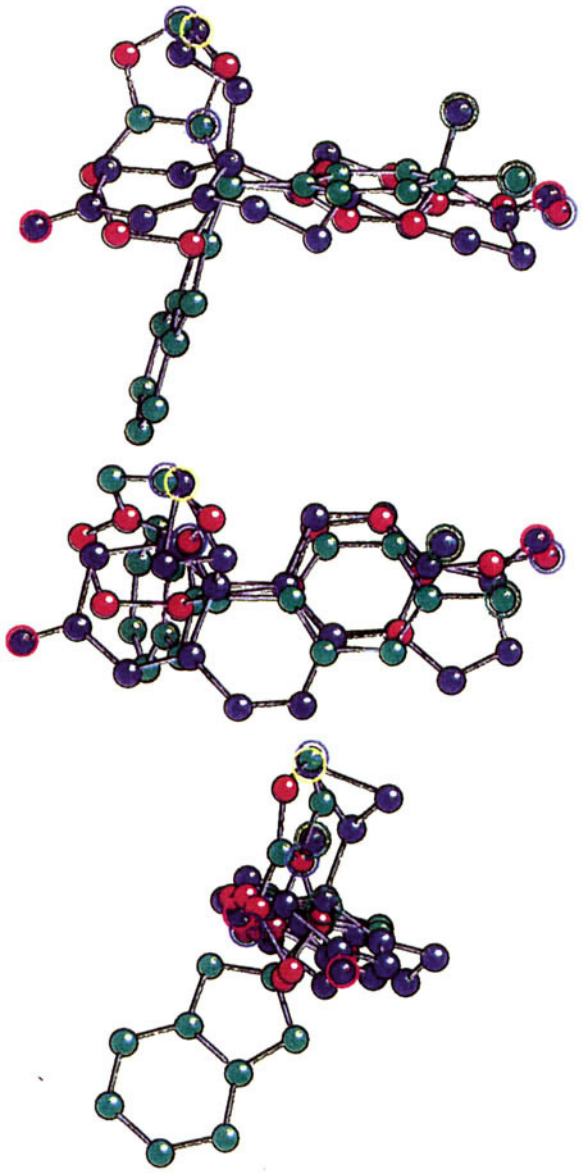

FIGURE 5 Superimposition of TAD (blue), (*S*)-(−)-fadrozole (red) and (*R*)-(**8**) (green). Atoms used for fitting: [N3 fad, N1 (*R*)-(**8**)]; C2, C2); (N1, N3); (C5, C4) and (C4, C5). Atom colours in circle: green (C), red (O), blue (N) and yellow (S).

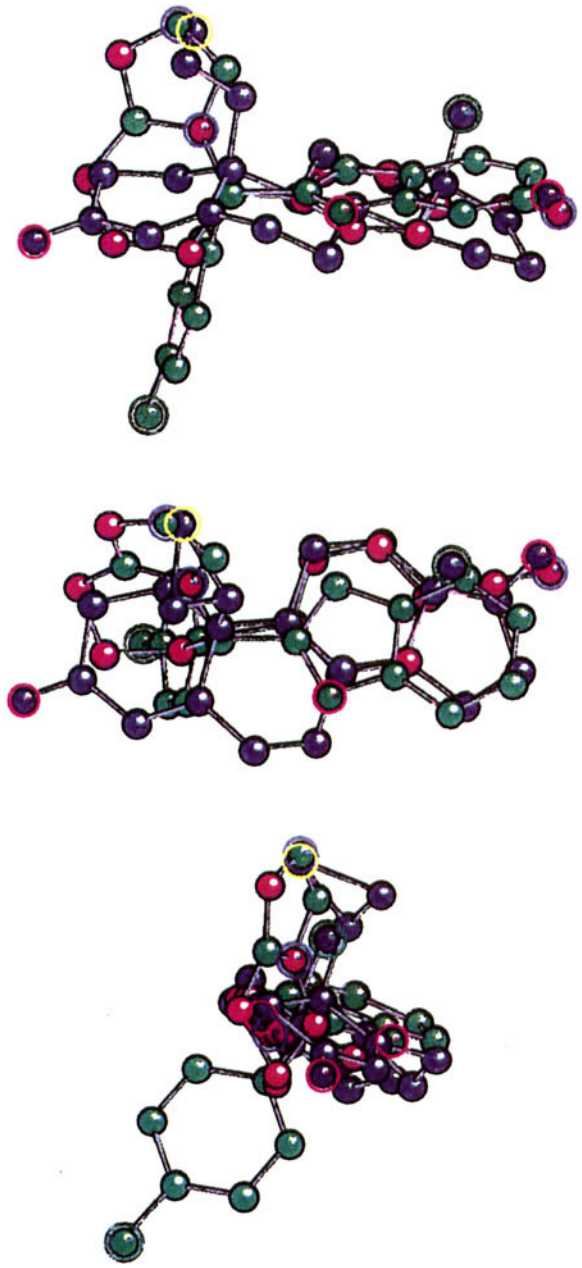

FIGURE 6 Superimposition of TAD (blue), (*S*)-(−)-fadrozole (red) and (*S*)-(8) (green). Atoms used for fitting; [N3 fad, N1 (*S*)-(8)]; (C2, C2); (N1, N3); (C5, C4) and (C4, C5). Atom colours in circle: green (C), red (O), blue (N) and yellow (S).

ring on the cyanophenyl of fadrozole and the phenyl ring dipped into the hydrophobic pocket. However, in both cases the imidazole functions were positioned in very close proximity to the imidazole ring of fadrozole. These results could account for the close activity (see Table I) of the (+)- and (−)-enantiomers of these three 1-[(benzofuran-2-yl)phenylmethyl]-1*H*-imidazoles described here. However, the model is too crude to rationalise the identical activity of the (+) and (−)-enantiomers of the 4′-chloro-analogue with the differences noted for the other two analogues.

### *Inhibitor Docking on Enzyme Active Site Model*

All of the calculations were performed using the AMBER suite of programs.[13] on Silicon Graphics Indigo workstations at the Institute of Cancer Research, Sutton, Surrey and the CRC Laboratories of Nottingham University. Visualisations were performed using the program MidasPlus from the Computer Graphics Laboratory, UCSF.[14] The candidate inhibitors were constructed using the Pimms program, minimised and optimised as described above. Partial atomic charges for the candidate inhibitors were calculated using MOPAC/ESP,[15] and missing forcefield parameters were obtained by interpolation from similar existing parameters. Minimisation of the protein-drug complexes was performed using the SANDER program from the AMBER suite to a root-mean square gradient of less than 0.1 kcal/mol/Å, using a non-bonded cut-off of 8 Å and keeping the protein backbone fixed. The interaction energies for the drug, protein and drug-protein complex were calculated using the ANAL module of AMBER. A $\Delta E_{binding}$ energy can then be obtained from:

$$\Delta E_{binding} = E_{inter} + \Delta E_{pert(drug)} + \Delta E_{pert(enzyme),} \quad (1)$$

where $E_{inter}$ is the drug/enzyme interaction energy, $\Delta E_{pert(drug)}$ the perturbation energy of the drug ($E^*_{drug} - E^\circ$), $\Delta E_{pert(enzyme)}$ is the perturbation energy of the enzyme ($E^*_{enz} - E^\circ_{enz}$).

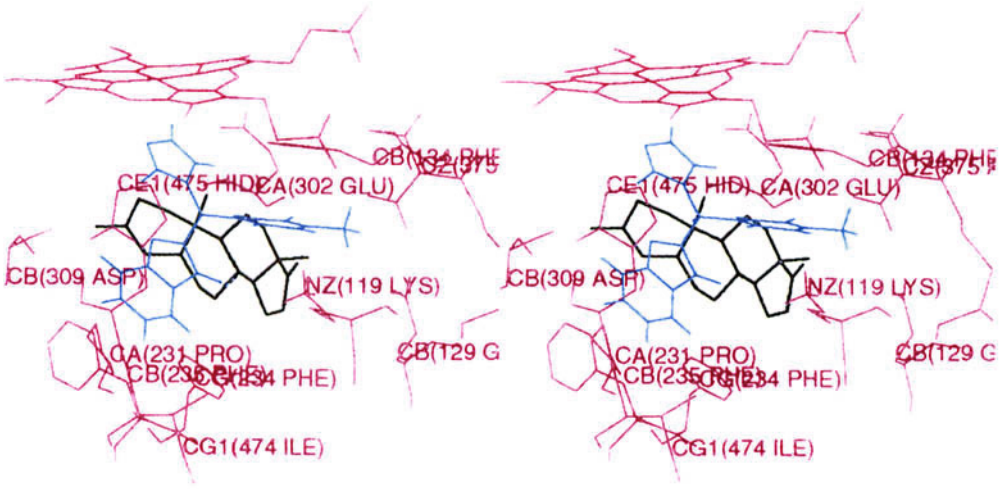


FIGURE 7 Stereoplot of the orientation of (*R*)-(**8**) in the active site model of aromatase. Heme (red), androstenedione (black), (*R*)-(**8**) (cyan) and some important residues (magenta).

(*R*)-(**8**), as representative of (**8–10**), was docked into the active site model of aromatase.[9] using the MidasPlus program. The proposed orientation of letrozole.[16,17] was used as a template and the imidazole of (*R*)-(**8**) was overlaid on the triazole of letrozole, the 4′-methylphenyl on the 4-cyanophenyl which is extended along the C and D rings of the steroid substrate and the benzofuran ring was superimposed on the other 4-cyano phenyl ring of letrozole, which is directed towards Asp-309 (N3-Fe of the heme was 2.35 Å). The complex of (*R*)-(**8**) and the aromatase model was then subjected to minimisation using the SANDER program by keeping the protein backbone fixed and the imidazole restrained but the protein side chains and other substituents of the inhibitor were allowed to move. After optimisation, the N3-Fe distance was 2.70 Å. The orientation of (*R*)-(**8**) in the active site of the model showed that the phenyl ring was positioned parallel to Phe-134, and the benzofuran near to Asp-309 and Phe-235 without any distortion (Fig. 7). The benzofuran oxygen was positioned towards the heme. To calculate the perturbation energies of the drug and the enzyme, energies of the enzyme $(E)^{\circ}_{enz}$ and the drug $((E)^{\circ}_{drug})$ in their ground state, (*R*)-(**8**) was translated to a position at least 15 Å distance from any of the amino acids residues of the enzyme model. The binding energy was then recalculated using the ANAL program to give $\Delta E_{binding} = -23.2$ kcal/mol.

(*S*)-(**8**) was similarly docked into the active site model by having the benzofuran ring extended along the C and D rings of the steroid substrate and the 4′-methylphenyl pointing towards Asp-309. The calculated binding energy was $\Delta E_{binding} = -23.2$ kcal/mol and the N3–Fe distance was 2.55Å. The orientation of (*S*)-(**8**) in the active site of the model after minimisation showed that the benzofuran was positioned parallel to Phe-134 near to Glu-302 and the phenyl ring was bound near to Asp-309 and Phe-235 without distortion (Fig. 8). The benzofuran oxygen was positioned towards Glu-302.

(*R*)-1-[(Benzofuran-2-yl)(4′-biphenyl)methyl]-1-*H*-imidazole (*R*-biphe), as a probe to establish possible steric bulk limitations of the enzyme binding sites, was similarly docked into the model and the biphenyl placed on the C and D ring of the substrate with as small as possible steric clash with the active site residues and the benzofuran pointing towards the Asp-309. (N3–Fe distance of 2.19 Å). Calculation gave

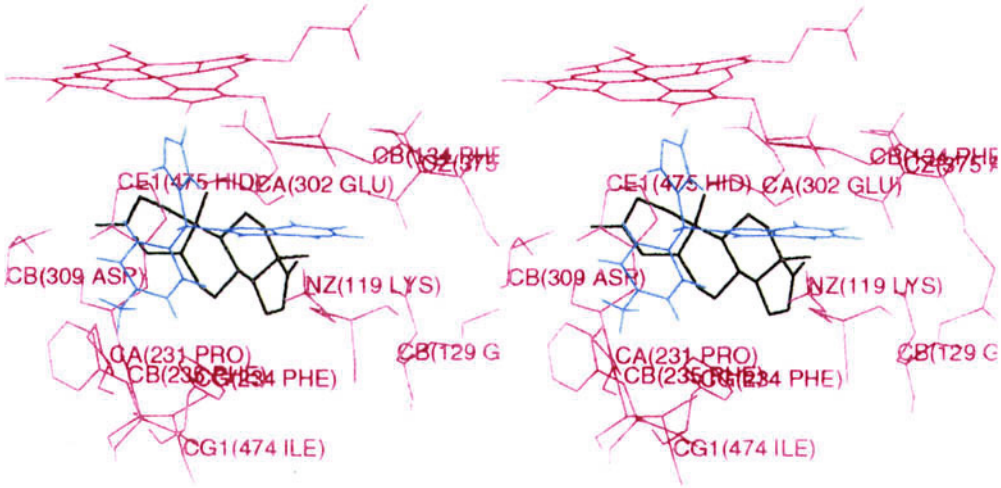


FIGURE 8 Stereoplot of the orientation of (*S*)-(**8**) in the active site model of aromatase. Heme (red), androstenedione (black), (*S*)-(**8**) (cyan) and some important residues (magenta).

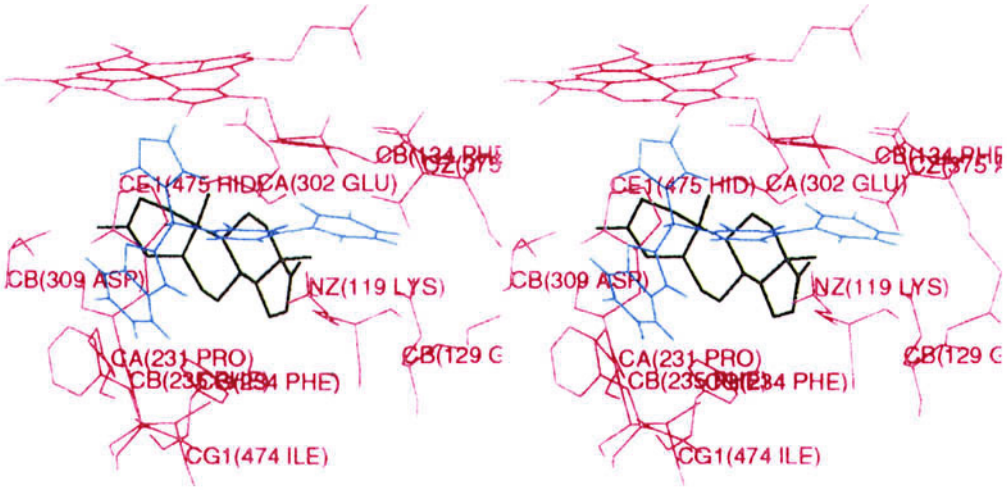


FIGURE 9 Stereoplot of the orientation of (*R*)-(biphe) in the active site model of aromatase. Heme (red), androstenedione (black), (*R*)-(biphe) (cyan) and some important residues (magenta).

$\Delta E_{binding} = -11.9$ kcal/mol. The orientation of (*R*)-(biphe) showed that the benzofuran ring was bound near Asp-309 with the oxygen pointing towards the heme and moved away from Phe-235. The biphenyl group was bent, the second phenyl group was twisted to be accommodated in the active site parallel to Phe-134 (Fig. 9).

(*S*)-1-[(Benzofuran-2-yl)(4′-biphenyl)methyl]-1-*H*-imidazole (*S*-biphe) was docked into the model so as to place the biphenyl on the *alpha*-face of the steroid substrate as described previously for (*S*)-(**8**) in an attempt to keep the orientation of (*S*)-(biphe) similar to that of fadrazole without any steric clash with the active site residues and the second phenyl was positioned in close proximity to Pro-231, Phe-234 and Phe-235. The calculation gave $\Delta E_{binding} = +14.1$ kcal/mol. The orientation of

(*S*)-(biphe) in the active site model showed that the compound was pushed down and towards the pocket which normally accommodates the C and D rings of the steroid substrate and the benzofuran was positioned parallel to Phe-134 with the oxygen pointed towards Glu-302. The biphenyl showed a very bad distortion and was bent away from Pro-231, Phe-234 and Phe-235 (Fig. 10). It seems that these amino acids prevent the accommodation of large residues on the alpha-face of the steroid substrate.

(*R*)-(+)-Fadrozole, the less active enantiomer, was docked into the active site model so as to place the 4-cyanophenyl in the active site pocket which normally accommodates the C and D rings of the substrate (N1–Fe(heme) = 2.29 Å). Calculation gave $\Delta E_{binding} = -4.1$ kcal/mol. The orientation of (*R*)-fadrazole in the model showed that the cyanophenyl group was accommodated on the C and D rings of the steroid substrate, parallel to Phe-134, and the piperidine was positioned on the A ring near to Asp-309 (Fig. 11).

(*S*)-(−)-Fadrozole, the more active enantiomer, was similarly docked into the model as described for the (*R*)-enantiomer (N1–Fe = 2.25 Å). Calculation gave $\Delta E_{binding} = -17.9$ kcal/mol. The orientation of (*S*)-(fadrozole) in the active site model showed the cyanophenyl bound on the C/D rings of the steroid, parallel to the Ph-134, and the piperidine ring bound on the A ring of the steroid near to Asp-309. (Fig. 12).

Docking of (*R*)-fadrozole and (*S*)-fadrozole into the active site model so as to position their cyanophenyl groups below the A ring of the substrate towards Asp-309 and the piperidine rings on the A ring of the steroid substrate gave calculated $\Delta E_{binding}$ values of +6.6 and +2.0 kcal/mol, respectively.

## DISCUSSION

As yet, the three dimensional structure of none of the eukaryotic P450 enzymes has been determined by X-ray crystallography due, in part, to their insoluble membrane-binding character, which inhibits their purification and crystallisation.[9] However, recently the crystal structure or rabbit P450 2C5 has been reported, though extensive protein engineering was required to produce a soluble form.[18] From the prokaryotic species, to date, only four bacterial P450 structures have been characterised by X-ray crystallography i.e. $P450_{cam}$ (P450 101),[19,20], P450BM-3 (P450 102),[21] P450terp (P450 108),[22]

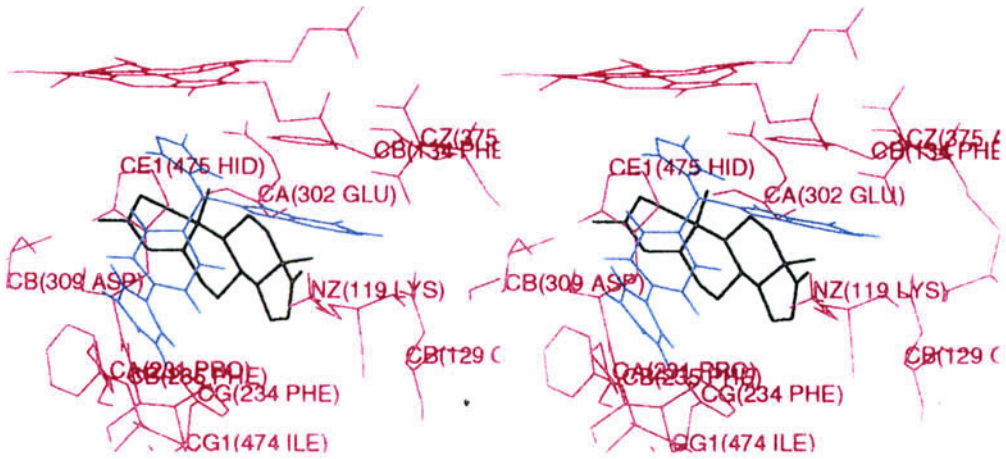


FIGURE 10 Stereoplot of the orientation of (*S*)-(biphe) in the active site model of aromatase. Heme (red), androstenedione (black), (*S*)-(biphe) (cyan) and some important residues (magenta).

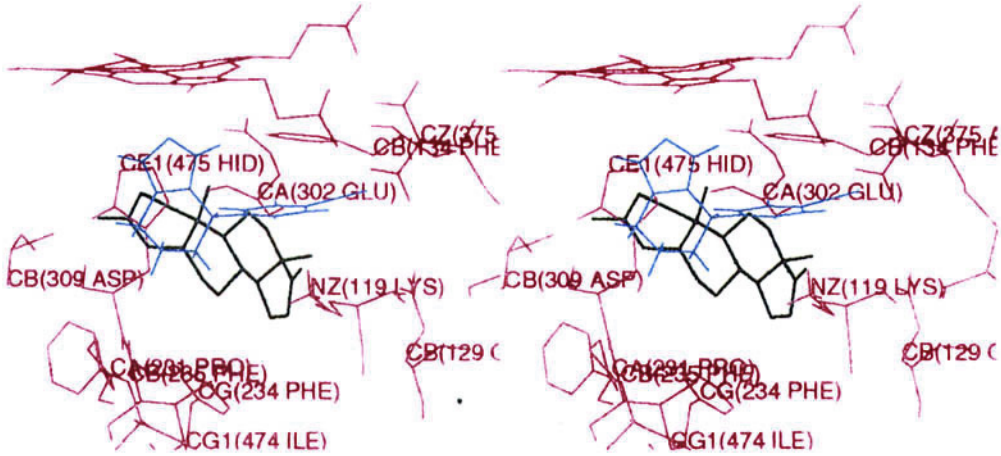


FIGURE 11 Stereoplot of the orientation of (*R*)-fadrozole in the active site model of aromatase. Heme (red), androstenedione (black), (*R*)-fadrozole (cyan) and some important residues (magenta).

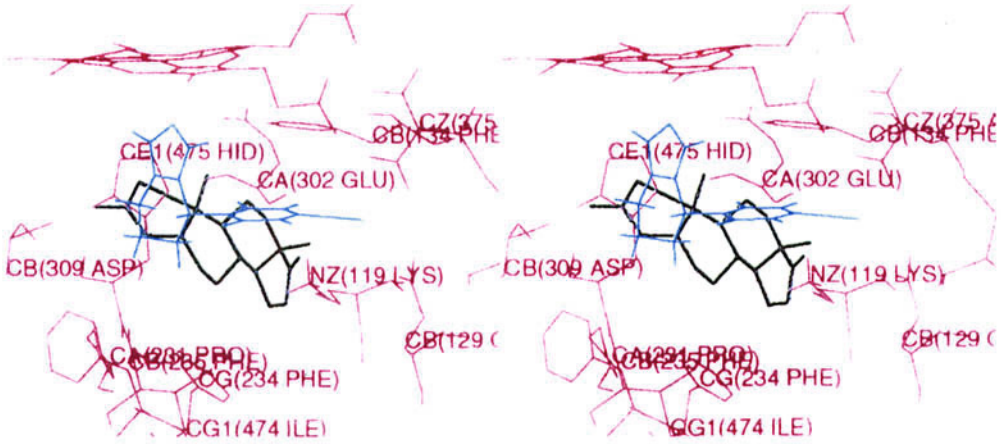


FIGURE 12 Stereoplot of the orientation of (*S*)-fadrozole in the active site model of aromatase. Heme (red), androstenedione (black), (*S*)-fadrozole (cyan) and some important residues (magenta).

and P450eryF.[23] Since the amino acid sequence of human placental aromatase has been described,[24–27] several structure-function studies have been carried out using site-directed mutagenesis.[16,17,28–30] Lack of information on the 3D-structure of human aromatase has encouraged several groups to propose models for the enzyme's active site.[9,16,17,31,32] Laughton *et al.*[9] have proposed a detailed three dimensional molecular model for human aromatase based on the crystal structure of P450cam[20] using sequence alignment, secondary structure prediction and molecular mechanics and dynamics, and have investigated the binding characteristics of some aromatase inhibitors on mutants previously described.[16,17]

The aim of the work undertaken here was to dock a 1-[(benzofuran-2-yl) phenylmethyl]-1*H*-imidazole and fadrozole into the active site of the aromatase model, predicted by Laughton *et al.*[9], and investigate their orientation in the active site as well as any steric requirements of

the site. (*R*)-, (*S*)-1-[(Benzofuran-2-yl) (4′-methylphenyl)methyl]-1*H*-imidazole (**8**) and (*R*)-, (*S*)-1-[(benzofuran-2-yl)(4′-biphenyl)methyl]-1-*H*-imidazole (biphe), the least active compound in this series ($IC_{50}$=242 nM, as its racemate;[33]), were chosen for the docking studies.

The inhibitors were then docked into the active site model, using the orientation of (*S*)-(−)-fadrozole[15] as a template, by having their imidazoles restrained towards the heme iron with a starting distance N3–Fe < 2.5 Å, the substituted phenyl of the (*R*)-enantiomers extended along one of the cyanophenyl rings of (*S*)-(−)-fadrozole i.e. rings C and D of the steroid substrate and the benzofuran rings pointed towards Asp-309. For the (*S*)-enantiomers, the benzofurans were positioned on the C and D rings of the substrate and the substituted phenyl rings placed near to Asp-309.

The $\Delta E_{\text{binding}}$ energies for (*R*)-(**8**) and (*S*)-(**8**) are −23.2 and −23.2 kcal/mol, respectively. Although the absolute configuration of the enantiomers of (**8**) are not yet known, the $IC_{50}$ values for the (+) and (−)-enantiomers of (**8**-DBT, see Table I, are 7.4 and 16.3 nM, respectively. That both are similarly and considerably potent aromatase inhibitors correlates well, if only qualitatively, with the modelling results.

The orientations of (*R*)-(**8**) and (*S*)-(**8**) in the model are shown in Figs. 7 and 8, respectively. The 4′-methylphenyl group of (*R*)-(**8**) is bound near (parallel) to Phe-134 and Glu-302 and the benzofuran ring binds near Asp-309 and Phe-235. The benzofuran oxygen was positioned towards the heme. However, docking of (*R*)-(**8**) by positioning the benzofuran oxygen in the opposite direction to the heme did not cause any reasonable change in the $\Delta E_{\text{binding}}$, $\Delta E_{\text{pert(enzyme)}}$ and $\Delta E_{\text{pert(drug)}}$ energies as well as the orientation of the drug in the active site (results are not included). For (*S*)-(**8**) the position of the phenyl and benzofuran rings are reversed i.e. the 4′-methylphenyl group binds near Asp-309 and Phe-235 and the benzofuran ring is bound near (parallel) to Phe-134 and Glu-302. The benzofuran oxygen was positioned towards Glu-302. There are no high values for $\Delta E_{\text{pert(enzyme)}}$ and $\Delta E_{\text{pert(drug)}}$ for both (*R*)-(**8**) an (*S*)-(**8**) but the $E_{\text{Inter}}$ for both enantiomers shows high negative values. This could be accounted for by good binding of these enantiomers in the active site without any major distortion of the drug or the enzyme.

The $\Delta E_{\text{Binding}}$ energies of (*R*)-, (*S*)-1[(benzofuran-2-yl)(4′-biphenyl)methyl]-1*H*-imidazole (biphe) are −11.9 and +14.1 kcal/mol, respectively. This overall increase in the $\Delta E_{\text{Binding}}$ energies was expected compared with (**8**) enantiomers, as the (biphe) racemate has an $IC_{50}$=242 nM, i.e. about 30 times less active than the racemates of (**8**).[33]

The orientation of (*R*)-(biphe) and (*S*)-(biphe) are shown in Figs. 9 and 10, respectively. The biphenyl ring of (*R*)-(biphe) was accommodated in the region of the C and D rings of the substrate. The phenyl rings were bent perhaps due to a steric clash with Phe-134. The whole molecule was pushed away from Phe-235 and Pro-231 perhaps due to a steric clash with this part of the active site which gave relatively high values for the $\Delta E_{\text{pert(enzyme)}}$ and $\Delta E_{\text{pert(drug)}}$ energies, although it has a very good $E_{\text{Inter}}$ energy. It seems that the normal pocket of the enzyme cannot accommodate long substituents such as the biphenyl group. The benzofuran ring was bound near Asp-309 and Phe-235. The benzofuran oxygen was positioned towards the heme, however, docking of (*R*)-(biphe) by positioning the benzofuran oxygen in the opposite direction to the heme did not cause any favourable change in the $\Delta E_{\text{Binding}}$, $\Delta E_{\text{pert(enzyme)}}$ and $\Delta E_{\text{pert(drug)}}$ energies as well as the orientation of the drug in the active site (results not included). Examination of Fig. 10 shows that (*S*)-(biphe) has its benzofuran bound parallel to Phe-134 and near to Glu-302 (the benzofuran oxygen positioned towards Glu-302) and the biphenyl is positioned towards Asp-309. The biphenyl ring is strongly tilted as the phenyl rings became non-planar and pushed away from Pro-231 and Phe-235. This

could account for the high $\Delta E_{pert(enzyme)}$, $\Delta E_{pert/drug)}$ and $\Delta E_{Binding}$ energies although it has a very good $E_{inter}$ energy. It seems that the proposed region under the A ring cannot accommodate large groups perhaps due to steric clashes with Pro-231, Phe-235 and Phe-234.

(*R*)- and (*S*)-Fadrozole were separately docked into the model so as to have their cyanophenyl groups on the C and D rings and the piperidine ring on the A ring of the steroid substrate (Figs. 11 and 12). There is a relatively good relationship between the $\Delta E_{Binding}$ energies (−4.1 and −17.9 kcal/mol), and the $IC_{50}$ values (680 and 3.8 nM.[8]) for the (*R*)- and (*S*)-enantiomers, respectively. The higher $\Delta E_{Binding}$ energy of (*R*)-fadrozole could be attributed to the high $\Delta E_{pert(enzyme)}$ energy. The cyanophenyl rings of both (*R*)-fadrozole and (*S*)-fadrozole were accommodated in the region of the C and D rings of the substrate parallel to Phe-134 and near to Glu-302 while the piperidine rings were positioned on the A ring of the substrate near to Asp-309, respectively. This orientation is in agreement with the orientation of (*S*)-fadrozole proposed by Furet *et al.*[8]

In another attempt (*R*)-fadrozole and (*S*)-fadrozole were separately docked into the active site model so as to have their cyanophenyl groups pointing below the A ring of the substrate towards Asp-309 and the piperidine rings on the A ring of the steroid substrate. In both cases poor binding energies were obtained (+6.624 and +1.149 kcal/mol for the (*R*)- and (*S*)-enantiomers, respectively). This finding is in contrast with the orientation of (*S*)-fadrozole proposed by Koymans *et al.*[31] who used a different model of aromatase.

The superimposition modelling studies, based on the model of Furet *et al.*,[8] together with the docking studies with the model of the active site of aromatase by Laughton *et al.*[9] using a series of potent 1-[benzofuran-2-yl)phenylmethyl]imidazoles lead to similar conclusions concerning the structural requirements for tight binding of azole inhibitors to the enzyme. This information may aid future design studies.

## *References*

[1] Brodie, A. (1994) "Design of Enzyme Inhibitors as Drugs", In: Sandler, M. and Smith, H.J., eds, (Oxford Science Publications, Oxford), pp 414–438.
[2] Kaye, B. (1991), *Biochem. Soc. Trans.* **19**, 456–459.
[3] Pepper, C.J., Smith, H.J., Nicholls, P.J., Barrell, K.J. and Hewlins, M.J.E. (1994), *Chirality* **6**, 400–404.
[4] Graves, P.E. and Salhanick, H.A. (1979), *Endocrinology* **105**, 52–57.
[5] Luscombe, D.K., Tucker, M., Pepper, C.J., Nicholls, P.J., Sandler, M. and Smith, H.J. (1994) "Design of Enzyme Inhibitors as Drugs", In: Sandler, M. and Smith, H.J., eds, (Oxford University Press, Oxford) **Vol. 2**, pp 1–41.
[6] Khodarahmi, G.A., Smith, H.J., Nicholls, P.J. and Ahmadi, M. (1998), *J. Pharm. Pharmacol.* **50**, 1321–1330.
[7] Whomsley, R., Fernandez, E., Nicholls, P.J., Smith, H.J., Lombardi, P. and Pestillini, V. (1993), *J. Steroid Biochem. Mol. Biol.* **44**, 675–676.
[8] Furet, P., Batzl, C., Bhatnager, A.S., Francotte, E., Rihs, G. and Lang, M. (1993), *J. Med. Chem.* **36**, 1393–1400.
[9] Laughton, C.A., Zvelebil, M.J.J.M. and Neidel, S. (1993), *J. Steroid Biochem. Mol. Biol.* **44**, 399–407.
[10] Pestillini, V., Giolitti, A., Pasqui, F., Abelli, L., Cutrufo, C., *et al.*, (1988), *Eur. J. Med. Chem.* **23**, 203–206.
[11] Pestillini, V., Gianotti, A., Giolitti, A., Fanto, N., Riviera, L. and Bellotti, M.G. (1987), *Chemioterapia* **6**, 269–271.
[12] Thompson, E.A. and Siiteri, P.K. (1974), *J. Biol. Chem.* **249**, 5373–5378.
[13] Pearlman, A.D., Case, D.A., Caldwell, J.C., Seibel, G.L., Chandra Singh, U., Weiner, P. and Kollman, P.A. (1991) AMBER 4.0 (University of California, San Francisco).
[14] Ferrin, T.E., Haung, C.C., Jarvis, L.E. and Langridge, R. (1988), *J. Mol. Graphics* **6**, 13–27.
[15] Stewart, J.P.P., Mopac 6.0 (QCPE), available from the Quantum Chemistry Programme Exchange, Indiana University, Bloomington, IN.
[16] Zhou, D.J., Cam, L.L., Laughton, C.A., Korzekwa, K.R. and Chen, S. (1994), *J. Biol. Chem.* **269**, 19501–19508.
[17] Kao, Y.C., Cam, L.L., Laughton, C.A., Zhou, D.J. and Chen, S.A. (1996), *Cancer Res.* **56**, 3451–3460.
[18] Williams, P.A., Cosme, J., Sridhar, V., Johnson, E.F. and McRee, D.E. (2000), *Mol. Cell.* **5**, 121.
[19] Poulos, T.L., Finzel, B.C., Gunsalus, I.C., Wagner, G.C. and Kraut, J. (1985), *J. Biol. Chem.* **260**, 16122–16130.
[20] Poulos, T.L. and Howard, A.J. (1987), *Biochemistry* **26**, 8165–8174.
[21] Ravichandran, K.G., Boddupalli, S.S., Hasemann, C.A., Peterson, J.A. and Deisenhofer, J. (1993), *Science* **261**, 731–736.
[22] Hasemann, C.A., Ravichandran, K.G., Peterson, J.A. and Deisenhofer, J. (1994), *J. Mol. Biol.* **236**, 1169–1185.
[23] Cupp-Vickery, J.R. and Poulos, T.L. (1995), *Struct. Biol.* **2**, 144–153.
[24] Harada, N. (1988), *Biochem. Biophys. Res. Commun.* **156**, 725–732.
[25] Corbin, C.J., Graham-Lorence, S., McPhaul, M., Mason, J.I., Mendelson, C.R. and Simpson, E.R. (1988), *Natl. Acad. Sci. USA* **85**, 8948–8952.
[26] Toda, K., Teashima, M., Mitsuuchi, Y., Yamasaki, Y., Yokoyama, Y., Najima, S., *et al.*, (1989), *FEBS Lett.* **247**, 371–376.

[27] Pompon, D., Liu, R.Y.K., Besman, M.J., Wang, P.L., Shively, J.E. and Chen, S. (1989), *Mol. Endocrinol.* **3**, 1477–1487.
[28] Zhou, D., Pompon, D. and Chen, S. (1991), *Proc. Natl. Acad. Sci. USA* **88**, 410–414.
[29] Zhou, D., Korzekw, K.R., Bulos, T. and Chen, S. (1992), *J. Biol. Chem.* **267**, 762–768.
[30] Zhou, D., Cam, L., Laughton, C.A., Korzekw, K.R. and Chen, S. (1994), *J. Biol. Chem.* **269**, 19501–19508.
[31] Koymans, L.M.H., Moereels, H. and Vanden Bossche, H. (1995), *J. Steroid Biochem. Mol. Biol.* **53**, 191–197.
[32] Kao, Y.C., Cam, L.L., Laughton, C.A., Zhou, D., Chen, S., unpublished work.
[33] Whomsley, R., private communication.